Optimal Energy Management System for Microgrids considering Energy Storage, Demand Response and Renewable Power Generation

Ayşe Kübra Erenoğlu[1], İbrahim Şengör[2,3], Ozan Erdinç[1], Akın Taşcıkaraoğlu[4], João P. S. Catalão[5,*]

[1] Electrical Engineering Department, Yıldız Technical University, İstanbul, Turkey

[2] Environmental Research Institute, MaREI, University College Cork, Cork, Ireland

[3] Electrical and Electronics Engineering Department, İzmir Katip Çelebi University, İzmir, Turkey

[4] Electrical and Electronics Engineering Department, Muğla Sıtkı Koçman University, Muğla, Turkey

[5] Faculty of Engineering of the University of Porto and INESC TEC, Porto 4200-465, Portugal

*Corresponding author at: catalao@fe.up.pt

Abstract: To ensure the autonomous power supply in MGs in stand-alone mode while also maintaining stability, energy storage systems (ESSs) and demand-side flexibility can be utilized together. Motivated by this fact, in this study, a scenario-based energy management system (EMS) modelled as a mixed-integer linear programming (MILP) problem is presented by taking the stochastic nature of wind and photovoltaic (PV) sources into account in order to analyze the operational behaviour of MGs and thereby to reduce the network energy losses. Direct load control (DLC) based demand response (DR) program is implemented to the system with the objective of exploiting the remarkable potential of thermostatically controllable appliances (TCAs) for energy reduction while satisfying comfort and operational constraints. Furthermore, a common ESS with a bi-directional power flow facility is incorporated in the proposed structure and electric vehicles (EVs) are employed as an additional flexible load in grid-to-vehicle (G2V) mode. To testify the effectiveness of the proposed optimization algorithm, different case studies are conducted considering diverse scenarios. Moreover, the performance is compared with a deterministic method from the perspective of achieving loss reduction and capturing the uncertainties.

Keywords: Demand side management; electric vehicle; microgrids; renewable generation; shared energy storage.

1. Introduction

1.1 Motivation and Background

Microgrids (MGs) are small-scale low-voltage energy systems that play an increasingly important role in the modern power grid, recently. These autonomous systems consist of modular and distributed generation (DG) units, energy storage systems (ESSs), and a cluster of local loads with distinct electrical boundaries [1]. MGs can be operated in either grid-connected or stand-alone mode effectively. In a grid-connected mode operation, a point of common coupling enables bi-directional power exchange, allowing energy to be fed from or injected into the upstream grid [2].

Apart from various benefits, the MG structure has also some problems in terms of high resistance losses due to the low operating voltage [3]. Besides, it is widely accepted that MGs currently rely on renewable energy systems (RESs) in energy generation instead of carbon-intensive energy sources due to environmental concerns [4]. However, the unpredictable nature of RESs brings about significant challenges in MG operation. Moreover, in addition to the fluctuation on the power supply side, electricity prices, end-users' demand, and heterogeneity of electric loads have also caused uncertainties for demand side. These changes becloud supply-demand equality and frequency/voltage stability in MGs [5].

The aforementioned major issues can be handled with various methods, such as employing ESSs, including controllable generating units, and integrating demand response (DR) programs into the operational tools to enhance the system's reliability and security. One of the well-known types of DR, the direct load control (DLC) based DR strategies are conducted for thermostatically controlled appliances (TCAs), such as refrigerators, air conditioners (ACs), and electric water heaters. These flexible loads are utilized as ancillary services for instantaneous changes in switching conditions due to their rapid response and thermal inertia [6].

It is evidently seen that modern MGs are complicated energy structures that integrate RESs, dispatchable generating units, different types of prosumers together with the heterogeneity of the appliances and ESSs. Therefore, the development of an energy management system (EMS) is an attractive solution and plays a critical role in long-term MG planning with coordinating above mentioned frameworks in order to enhance the system performance. Also, there is an opportunity to provide sustainable energy to the end-users thanks to DR programs by mitigating power imbalances associated with intermittent RESs.

1.2 Relevant Background

Various methods are available in the literature for modelling MG's complicated architecture to accomplish technical, economic, and environmental benefits associated with MG deployment. Most of the existing studies are concentrated on deterministic-based mathematical frameworks [7, 8] in which it is possible to determine the output value by the given parameters and initial conditions [9]. Although the deterministic approach is evaluated as one of the widely-used techniques in MG operation [10], consideration of uncertainties has attracted great interest from the academic community and industry. In this sense, different methodologies have been introduced for uncertainty management in the operating of a traditional distribution system and/or MG.

Stochastic techniques [11]-[12], sensitivity analysis [13]-[14], and fuzzy modelling approaches [15]-[16] have been broadly used methods in the literature for dealing with various unpredictable natural phenomena. Natural variability is considered as uncertainties [17] in sensitivity analysis, on the other hand, membership functions are identified in fuzzy modelling based on the personal experiences [18]. Hence, it is important to emphasize that a stochastic methodology is superior to others when comparing the benefits and drawbacks of the aforementioned techniques.

It has become one of the most widely-used schemes for not only energy management systems but also transportation models, logistics, financial instruments, and network design [19]. In essence, the intermittent nature of RESs can be addressed in the MG concept by creating numerous scenarios that ensure a probabilistic guarantee for constraint satisfaction [20] and also taking into account worst-case situations [10].

The number of studies in the literature on EMS strategies that take various combined structures into account for providing optimal MG operation has increased recently. Table 1 provides a comprehensive classification of specialized literature in the proposed research area. Although the DR is foreseen to be an essential part of MGs operations, the literature studies [13]-[33] did not take it into consideration together with EV integration. It should be underlined that neither any type of DR implementation nor EV integration was taken into account in [34], [38]-[40]. Also, the models in [38]-[40] disregard the power flow constraints, while optimizing their decision making algorithms. Furthermore, a non-convex mixed integer nonlinear program based model was presented in [38] which does not guarantee global optimality. In addition, uncertainties due mainly to RESs were not even touched in [39]. On the other hand, the price-based demand response (PBDR) program was the issue in [35]-[37], [41] while the most effective demand reduction application, DLC-based DR was neglected.

It can be deduced from the taxonomy table that this study has some crucial differences from the existing literature, especially considering uncertainty handling method, DR implementation, optimal power flow tool, and objective function. Collaborated operation of DLC-based DR program, RESs-based distributed power generation units, EV, and common ESS has been provided under the effective energy management system framework.

1.3 Contributions and Organization of the Paper

It can be stated that the uncertain generation of wind and PV along with the power flow analysis have been neglected in the most recent literature according to the comprehensive review. Considering this fact, a scenario-based stochastic optimization framework is presented in this study by incorporating multivariant participants (industrial, commercial and residential) together with controllable and non-controllable appliances in MG with the aim of maximizing total loss reduction. The detailed MILP-based mathematical model makes it possible to ensure global optimality.

Table 1: Classification of specialized literature in the proposed research area

Ref.	RES	DR	ESS	EV	Type of End-user			Power Flow	Method of Component Modelling						Mode of Operation		Objective Function
					Res.	Com.	Ind.		Det.	Rob.	Sensitivity Analysis	Stochastic Approach	Fuzzy Model	Mixture	Grid-connected	Stand-alone	
[13]	✔	✘	✔	✘	N/A	N/A	N/A	✘	✘	✘	✔	✘	✘	✘	✔	✘	Cost optimization
[14]	✔	✘	✔	✘	✔	✘	✘	✘	✘	✘	✔	✘	✘	✘	✘	✔	Cost optimization
[15]	✔	✘	✔	✘	N/A	N/A	N/A	✘	✘	✘	✘	✘	✔	✘	✔	✘	Minimizing operating costs&fossil fuel consumption
[16]	✔	✘	✔	✘	✔	✘	✘	✘	✘	✘	✘	✘	✔	✘	✘	✔	Minimizing the operational cost
[21]	✔	✘	✔	✘	N/A	N/A	N/A	✔	✔	✘	✘	✘	✘	✘	✘	✔	Minimizing capital investment&fuel costs
[22]	✔	✔	✔	✘	N/A	N/A	N/A	✔	✔	✘	✘	✘	✘	✘	✔	✔	Minimizing total cost&comfort
[23]	✔	✘	✔	✘	N/A	N/A	N/A	✔	✘	✘	✘	✔	✘	✘	✘	✔	Minimizing operating costs&pollutant emissions
[24]	✔	✘	✔	✘	N/A	N/A	N/A	✔	✘	✘	✘	✔	✘	✘	✔	✘	Minimizing fuel&operation&losses cost
[25]	✔	✘	✔	✘	N/A	N/A	N/A	✔	✔	✘	✘	✘	✔	✔	✔	✔	Minimizing operating cost&enviromental impact
[26]	✔	✘	✔	✘	✔	✘	✘	✔	✔	✘	✘	✘	✘	✘	✔	✘	Minimizing electricity grid losses
[27]	✔	✔	✘	✘	✔	✔	✔	✘	✔	✘	✘	✘	✘	✘	✘	✔	Cost minimization
[28]	✔	✔	✘	✘	✔	✔	✔	✔	✔	✘	✘	✘	✘	✘	✔	✘	Cost minimization
[29]	✔	✔	✔	✘	✘	✔	✘	✘	✔	✘	✘	✘	✘	✘	✔	✘	Peak load reduction&cost minimization
[30]	✔	✔	✔	✘	✔	✘	✘	✘	✘	✘	✘	✘	✘	✔	✘	✔	Cost&emission minimization
[31]	✔	✔	✘	✘	✔	✔	✔	✔	✔	✘	✘	✘	✘	✘	✔	✘	Minimizing MG operational cost
[32]	✔	✔	✔	✘	N/A	N/A	N/A	✘	✔	✘	✘	✘	✘	✘	✔	✘	Minimizing the operational cost
[33]	✔	✔	✔	✘	✔	✔	✔	✘	✔	✘	✘	✘	✘	✘	✘	✔	Minimizing total cost
[34]	✔	✘	✔	✘	N/A	N/A	N/A	✔	✘	✔	✘	✘	✘	✘	✔	✘	Cost minimization
[35]	✔	✔	✔	✘	N/A	N/A	N/A	✘	✘	✘	✘	✘	✘	✔	✔	✘	Optimization of cost&emission
[36]	✔	✔	✔	✘	N/A	N/A	N/A	✔	✘	✘	✘	✔	✘	✘	✘	✔	Cost minimization
[37]	✔	✔	✔	✘	✔	✘	✘	✘	✘	✘	✘	✔	✘	✘	✔	✘	Cost minimization
[38]	✔	✘	✔	✘	✔	✔	✘	✘	✔	✘	✘	✘	✘	✘	✘	✔	Cost&emission minimization
[39]	✔	✘	✔	✘	✔	✔	✔	✘	✔	✘	✘	✘	✘	✘	✔	✘	Maximizing the profit
[40]	✔	✘	✔	✘	✔	✔	✘	✘	✔	✘	✔	✘	✘	✔	✘	✔	Cost optimization
[41]	✔	✔	✔	✘	N/A	N/A	N/A	✘	✘	✘	✘	✔	✘	✘	✔	✘	Cost minimization
This Study	✔	✔	✔	✔	✔	✔	✔	✔	✔	✘	✘	✔	✘	✔	✔	✘	Minimizing distribution grid losses

Note: N/A=Not Available, RES=Renewable Energy Source, DR= Demand Response, ESS=Energy Storage System, EV=Electric Vehicle, Res=Residential end-user, Com=Commercial end-user, Ind= Industrial end-user, Det=Deterministic, Rob= Robust

The major contributions of this study are as follows:

1) Flexibility provisioning through a DLC-based DR program that allows more efficient energy management by utilizing the gathered flexibility in loss minimization and performance enhancement of the MG is considered in the proposed scheme. The thermal model enables to alteration of the power profiles of the thermostatically manageable loads while still satisfying the requirements of temperature ranges.

2) The intermittency associated with the RES generation, namely wind and PV farms is dealt with scenario-based system modelling in a stochastic day-ahead planning context, which has been rarely considered in the literature. The detailed framework provides coordinated operation of EVs alongside the dynamic component of ESS and RESs.

3) The performance of the proposed stochastic model is compared with the deterministic method by simulation validation under several case studies to demonstrate the effectiveness of the proposed scenario-based EMS framework on the considered multi-component MG structure.

The remainder of the paper is organized as follows: Section 2 presents the mathematical basis of the generation and ESS units, and also all operational possibilities in the MG structure. Afterward, Section 3 includes the case studies for evaluating the effectiveness of the proposed scheme and, finally, Section 4 draws the conclusions.

2. Problem Formulation

2.1 General Scheme of the Proposed Framework

The demonstration of the proposed MG structure that has bi-directional power flow capability is shown in Fig. 1. The demand of this MG is provided by the upstream grid and/or locally distributed power sources. The surplus energy may be stored in a shared storage system and/or injected into the upstream grid by means of optimal MG operation. Industrial, commercial and residential end users are considered in this structure. To address the uncertainties, a scenario-based stochastic optimization approach is proposed.

2.2 Mathematical Formulation

This subsection elucidates the mathematical formulation of MILP-based EMS together with the system operational constraints and power flow.

2.2.1 Objective Function

Aiming at minimizing the total losses in MG, an objective function given by (1) is proposed. To calculate total losses during the whole simulation period in a stochastic manner, $P_{b,v,w,t}^{loss}$ should be multiplied with equal probabilities of PV and wind scenarios (π_v, π_w).

$Minimize\ Losses$

$$\sum_{t}\sum_{b}\sum_{v}\sum_{w} \pi_v \cdot \pi_w \cdot P_{b,v,w,t}^{loss} \ , \forall b \in B, t \in T, \forall v, w \tag{1}$$

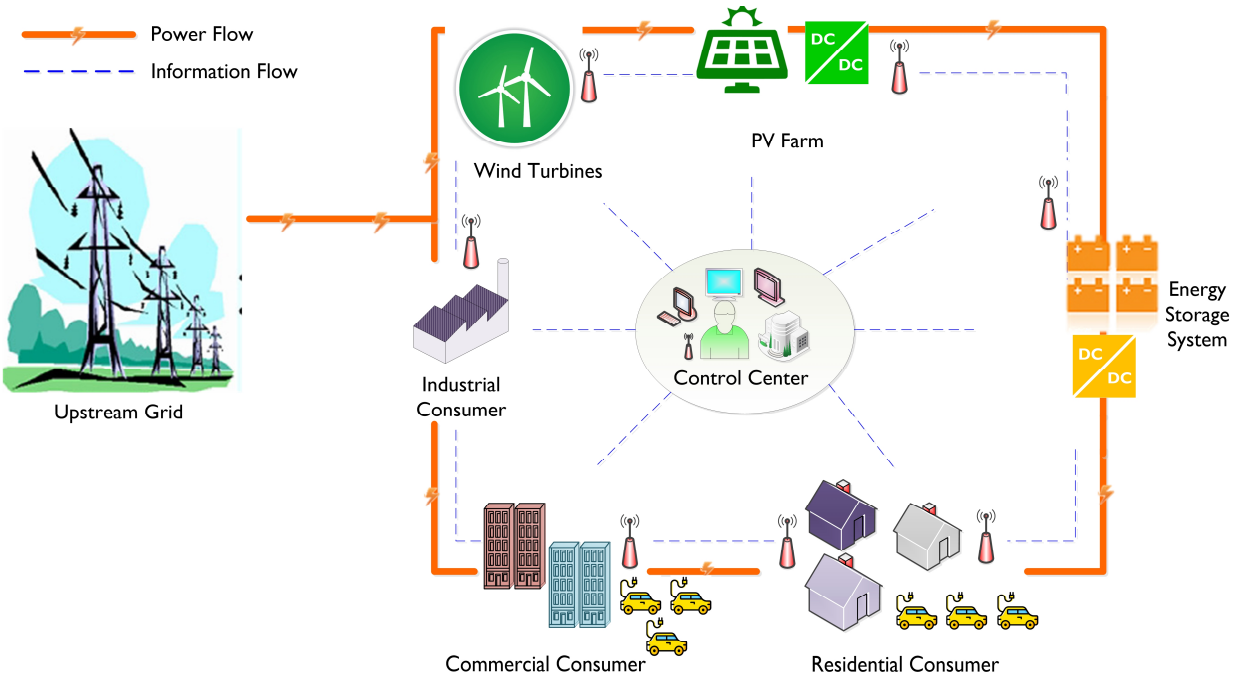

Fig. 1. Proposed smart microgrid structure.

2.2.2 Power Balance, Limits of Branch Flow and Substation

$$P_{v,t}^{pv,tot} + P_{w,t}^{wind,tot} + P_{v,w,t}^{ESS,dis,tot} + P_{i,v,w,t}^{f,load} + \sum_{b\in B:i\in\Omega_b^j} f_{b,v,w,t} - \sum_{b\in B:i\in\Omega_b^i} f_{b,v,w,t}$$

$$= P_{v,w,t}^{R,tot} + P_{v,w,t}^{C,tot} + P_t^{ind} + P_{v,w,t}^{ESS,ch,tot} \quad \forall i \in I, \forall t \in T, \forall v, w \tag{2}$$

$$-f_b^{max} \le f_{b,v,w,t} \le f_b^{max} \quad \forall b \in B, t \in T, \forall v, w \tag{3}$$

$$P_{i,v,w,t}^{f} = P_{i,v,w,t}^{f,load} + \sum_{b\in B} P_{b,v,w,t}^{loss} + P_{v,w,t}^{sell,grid} \quad \forall i \in \Omega_i^f, \forall t \in T, \forall v, w \tag{4}$$

$$P_{i,v,w,t}^{f} \le N \cdot u_{v,w,t}^{grid} \tag{5}$$

$$P_{v,w,t}^{sell,grid} \le N \cdot (1 - u_{v,w,t}^{grid}) \tag{6}$$

$$0 \le P_{i,v,w,t}^{f} \le P_i^{f,max} \quad \forall i \in \Omega_i^f, \forall t \in T, \forall v, w \tag{7}$$

In this MG architecture, the general power balance formulation is stated in (2) which is important to match supply and demand in every single period. Total produced power by renewable-based DG units, actual power provided by ESS discharging, and the transferred power from the upstream grid for meeting demand are represented on the supply side.

From the demand side perspective, total residential consumption including inflexible demand, flexible demand, and possessed EV charging power, commercial end-users' total consumption including inflexible demand, flexible demand, and EV charging power and industrial premise inflexible load are taken into consideration. Also, herein the total ESS charging power should be considered for the scenario v and w during the period t. Moreover, the power which flows from bus i to bus j (mirror set of nodes) and is sent to load busses from slack bus i are included in (2) by representing as $\sum_{b\in B:i\in\Omega_b^j} f_{b,v,w,t}$, $\sum_{b\in B:i\in\Omega_b^i} f_{b,v,w,t}$, respectively.

In this formulation, it should be highlighted that $b \in B: i \in \Omega_b^j$ in summation $\sum_{b\in B:i\in\Omega_b^j} f_{b,v,w,t}$ indicates flowing active power from bus j to i; while $\sum_{b\in B:i\in\Omega_b^i} f_{b,v,w,t}$ states leaving power from bus i.

The flowing power can be positive or negative depending on the optimal solution of the problem and this should be maintained between maximum branch flow limits as indicated in (3). Also, the load demand of busses, as well as power losses, should be covered by the upstream grid as stated in (4) by also taking into selling option account. However, it is not possible to draw/inject energy from/to the upstream grid simultaneously. Therefore, binary variable ($u_{v,w,t}^{grid}$) is necessary in the mathematical model in order to determine power transactions between upstream grid and MG by inequalities (5) and (6). Finally, (7) enforces the fact that a range of injected power from the upstream grid cannot exceed the specified constraint ($P_i^{f,max}$).

2.2.3 Linear Approximation of the Losses

$$P_{b,v,w,t}^{loss} = b \cdot \left|f_{b,v,w,t}\right| + c \cdot {f_{b,v,w,t}}^2 \quad \forall b \in B, \forall t \in T, \forall v, w \tag{8}$$

$$\sum_{p\in P} z_{b,v,w,t,p} = 1 \quad \forall b \in B, \forall t \in T \tag{9}$$

$$f_{b,v,w,t} = \sum_{p\in P} X_p \cdot z_{b,v,w,t,p} \quad \forall b \in B, \forall t \in T \tag{10}$$

$$F_{b,v,w,t} = \sum_{p\in P} Y_p \cdot z_{b,v,w,t,p} \quad \forall b \in B, \forall t \in T \tag{11}$$

Equation (8) expresses the power losses on a branch which is approximated using a second-order function of power flow in the lines multiplying with the coefficients q and j. It is clearly evident that this statement is not appropriate for MILP formulation due to its nonlinear characteristic. Thus, the Special Order Sets of Type 2 (SOS2) technique is considered in the linearization process as denoted in Eqs. (9)-(11). SOS2 has computational advantages. It is highlighted in the literature that the technique of SOS2 has minor approximation errors in linearization enabling the model of the system accurately.

2.2.4 DG Production

$$P_{v,t}^{pv,tot} = \sum_f P_{f,v,t}^{pv} \tag{12}$$

$$P_{w,t}^{wind,tot} = \sum_c P_{c,w,t}^{wind} \tag{13}$$

Equations (12) and (13) denote the total power production by PV farms in scenario v during period t and wind turbines in scenario w during period t, respectively. It is considered that there are two PV farms indicating f_1 and f_2 subsets while wind plants are c_1 and c_2.

3.2.5 Residential Model

$$P_{v,w,t}^{R,tot} = \sum_k \sum_h P_{k,h,v,w,t}^{R} \tag{14}$$

$$P^{R}_{k,h,v,w,t} = P^{inf,R}_{k,h,t} + P^{R,AC}_{k,h,v,w,t} + P^{EV,R}_{k,h,v,w,t} \quad (15)$$

The total residential consumption is shown in (14) and its inflexible demand, flexible demand, and EV charging power in scenarios v and w are denoted by (15).

2.2.5.1. Residential AC Model

$$T^{r,R}_{k,h,v,w,t} = \left(1 - \frac{\Delta t}{1000 \cdot M^{R}_{a} \cdot c_{a} \cdot R^{eq}_{k,h}}\right) \cdot T^{r,R}_{k,h,v,w,t-1} + \frac{\Delta t}{1000 \cdot M^{R}_{a} \cdot c_{a} \cdot R^{eq}_{k,h}} \cdot T^{a}_{t-1} - u^{R,AC}_{k,h,v,w,t-1} \frac{COP_{k,h} \cdot P^{R,AC}_{k,h} \cdot \Delta t}{0.000277 \cdot M^{R}_{a} \cdot c_{a}} \; \forall t > 1, \forall v, w \quad (16)$$

$$SP^{R,AC}_{k,h,t} - S^{R,d}_{v,w,t} \leq T^{r,R}_{k,h,v,w,t} \leq SP^{R,AC}_{k,h,t} + S^{R,u}_{v,w,t} \quad \forall t: SP^{R,AC}_{k,h,t} \neq NaN \quad (17)$$

$$P^{R,AC}_{k,h,v,w,t} = P^{R,AC}_{k,h} \cdot u^{R,AC}_{k,h,v,w,t} \quad (18)$$

$$T^{R,des}_{k,h} - T^{R,d}_{k,h} \leq T^{r,R}_{k,h,v,w,t} \leq T^{R,des}_{k,h} + T^{R,u}_{k,h} \quad \forall t \in [t_1, t_2], \forall v, w \quad (19)$$

The model depending on thermodynamic properties of materials and air, outdoor temperature, etc. is derived and expressed by (16)–(18). The indoor temperature limits are determined by the occupants and up/down variation of the temperature from the ideal point represented as positive $S^{R,u}_{v,w,t}$, $S^{R,d}_{v,w,t}$ variables respectively. These mentioned constraints are written for the thermostat set-point control mechanism (TSCM) method. Inequality (19) denotes the room temperature up/down limitations determined by end-users during DR horizon. With respect to these constraints, MG operator can switch on/off AC by direct compressor control mechanism (DCCM). Finally, the amount of energy consumption can be calculated using (18). Inside mass of air and equivalent house thermal resistances are used to control the power consumption of their possessed AC. These expressions are calculated from different formulas derived from [42].

2.2.5.2 Residential EV Model

$$0 \leq P^{EV,R}_{k,h,v,w,t} \leq R^{EV,R}_{k,h} \cdot u^{EV,R}_{k,h,v,w,t}, \quad \forall t \in [T^{a}_{k,h,r}, T^{d}_{k,h,r}] \quad (20)$$

$$SOE^{R}_{k,h,v,w,t} = SOE^{ini,R}_{k,h} + CE^{EV,R}_{k,h} \cdot P^{EV,R}_{k,h,v,w,t} \cdot \Delta t, \quad if\ t = T^{a}_{k,h,r} \quad (21)$$

$$SOE^{R}_{k,h,v,w,t} = SOE^{R}_{k,h,v,w,t-1} + CE^{EV,R}_{k,h} \cdot P^{EV,R}_{k,h,v,w,t} \cdot \Delta t, \quad \forall t \in (T^{a}_{k,h,r}, T^{d}_{k,h,r}] \quad (22)$$

$$SOE^{min,R}_{k,h} \leq SOE^{R}_{k,h,v,w,t} \leq SOE^{max,R}_{k,h}, \quad \forall t \in [T^{a}_{k,h,r}, T^{d}_{k,h,r}] \quad (23)$$

$$SOE^{R}_{k,h,v,w,t} = SOE^{max,R}_{k,h}, \quad if\ t = T^{d}_{k,h,r} \quad (24)$$

For each residential end-user, EV is formulated in (20)-(24). It should be noted that the Vehicle-to-Grid (V2G) operation is not taken into account in this study. The EV charging limits are given by (20). Taking the battery's specifications as well as arrival and departure times into account, the EV's state-of-energy (SOE) is defined in (21) and (22). For limiting the bounds of SOE in order to avoid over-charging and deep-discharging, inequality (23) is defined. In (24), it should be underlined that before the departure of occupants, EVs should be fully charged.

2.2.6. Commercial Model

$$P_{v,w,t}^{C,tot} = \sum_l P_{l,v,w,t}^{C} \quad (25)$$

$$P_{l,v,w,t}^{C} = P_{l,t}^{inf,C} + P_{l,v,w,t}^{C,AC} + P_{l,v,w,t}^{EV,C} \quad (26)$$

The power demand of each commercial end-user including inflexible load, flexible load, and EV charging power is denoted by (26). It is to be highlighted that commercial end-users' EV and AC models can be derived from those of residential end users. Therefore, their formulation is not explained in this subsection considering paper length limitations.

2.2.7. ESS Model

$$P_{v,w,t}^{ESS,dis,tot} = P_{v,w,t}^{ESS,dis} \cdot DE^{ESS} \qquad \forall t, \mathrm{v}, \mathrm{w} \quad (27)$$

$$P_{v,w,t}^{ESS,ch,tot} = P_{v,w,t}^{ESS,ch} \cdot CE^{ESS} \qquad \forall t, v, w \quad (28)$$

$$0 \le P_{v,w,t}^{ESS,ch} \le R^{ESS,ch} \cdot u_{v,w,t}^{ESS} \qquad \forall t, v, w \quad (29)$$

$$0 \le P_{v,w,t}^{ESS,dis} \le R^{ESS,dis} \cdot \left(1 - u_{v,w,t}^{ESS}\right) \ \forall t, v, w \quad (30)$$

$$SOE_{v,w,t}^{ESS} = SOE_{v,w,t-1}^{ESS} + CE^{ESS} \cdot P_{v,w,t}^{ESS,ch} \cdot \Delta t - DE^{ESS} \cdot P_{v,w,t}^{ESS,dis} \cdot \Delta t, t \ge 1 \quad (31)$$

$$SOE_{v,w,t}^{ESS} = SOE^{ESS,ini} \quad , if \ t = 1 \quad (32)$$

$$SOE^{ESS,min} \le SOE_t^{ESS} \le SOE^{ESS,max} \quad \forall t \quad (33)$$

The ESS operation for MG is represented by (27)-(33) and has similar characteristics of the EV model explained before. However, ESS discharging option is also considered in order to provide energy to MG or injected to the upstream grid during energy shortages or peak periods. The other difference is that ESS is always available in MG as energy storage and can be charged or discharged at any time. It should be noted that binary variable $u_{v,w,t}^{ESS}$ is used for preventing charging and discharging of ESS at the same time interval.

3. Test and Results

A centralized loss reduction maximization oriented energy management system is modelled in the scope of the study. The main target of the developed framework is to investigate the impacts of the flexible sources on the distribution system operation from different perspectives. With the aim of minimizing the line losses in the branches during optimal operation of grid-connected MG, the propounded MILP model is tested in GAMS v.24.1.3 with CPLEX v.12 solver. With incorporating uncertain behaviour of wind turbines and PV farms, stochastic optimization-based strategy is taken into consideration.

To evaluate the effectiveness of the proposed methodology, the problem is solved by using a computer with a 2.3 GHz CPU and 32 GB RAM. The input data and related results from the different case studies will be discussed in the following subsections, respectively.

3.1 Input Data

The time granularity is chosen as 5 mins (0.0833h) in this study. The sample system with five nodes that have DGs, common ESS, and different types of end-users at different nodes as shown in Fig. 2 is derived from [43] to investigate the operational behaviour of the EMS. It should be reminded that the upstream grid-connection is provided by Node 1; PV farms and the commercial end-users have link with Node 2; common ESS is supposed to be connected at Node 3; industrial end-user and two wind turbines are connected from Node 4 and lastly, different types of all houses are connected from Node 5. Active power loss coefficients are 0.001 and 0.0003 MW^{-1}, and branches maximum power capacity was defined to be 3 MW [43]. Three end-user types (i.e., industrial, commercial and residential) are assumed to exist in the MG structure, and also, each end-user is equipped with non-controllable appliances whereas some end-users (commercial, residential) possess flexible appliances and EVs.

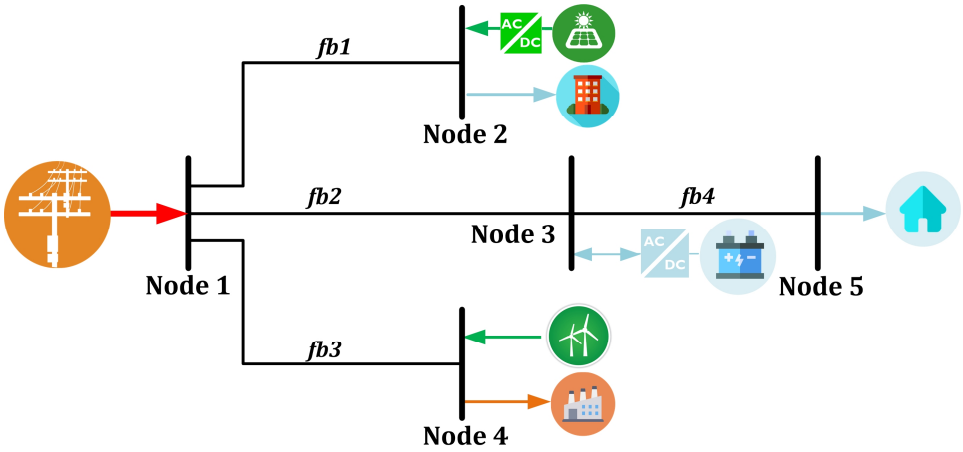

Fig. 2. The considered distribution system including 5 nodes.

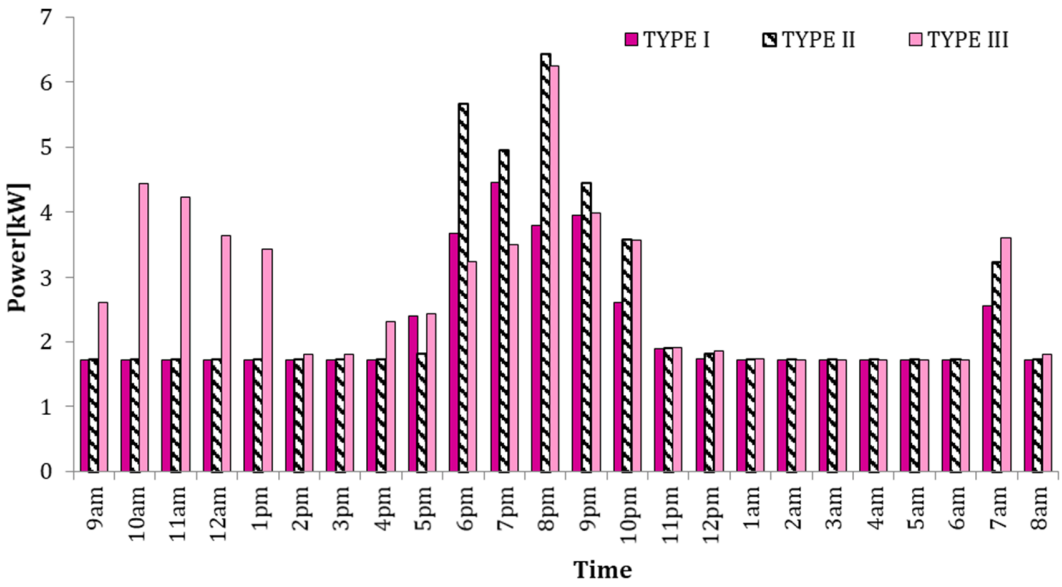

Fig. 3. Daily inflexible demand belonging to different types of residential end users.

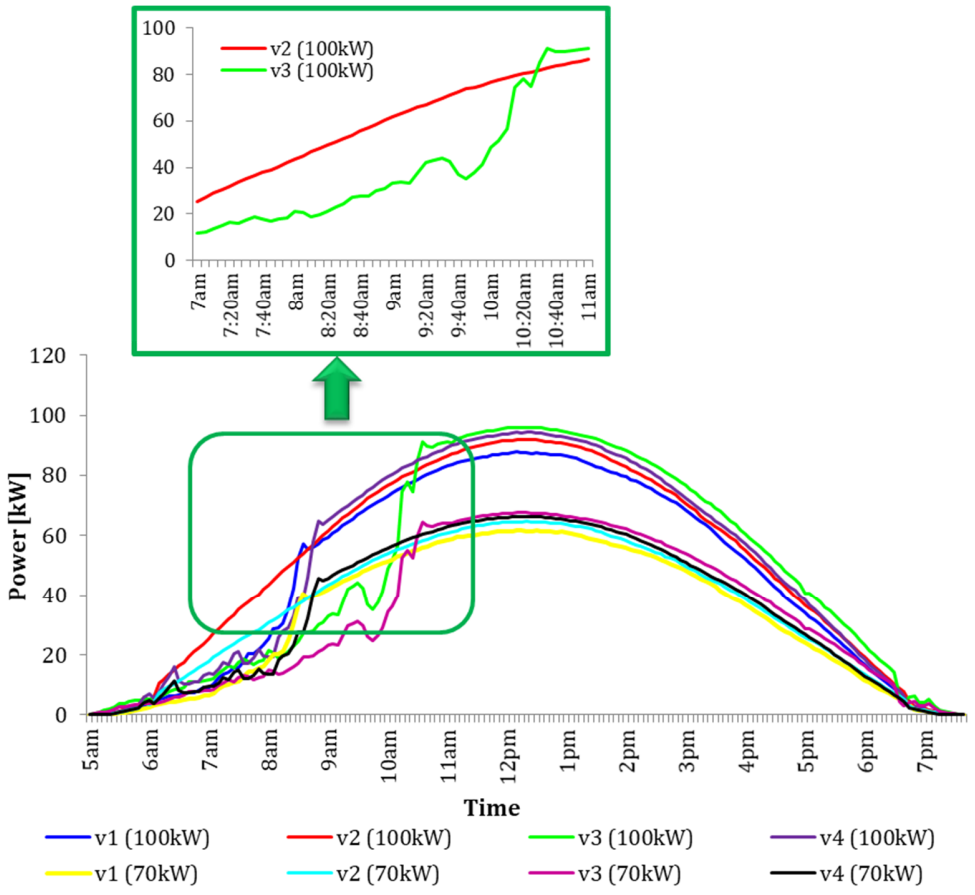

(a)

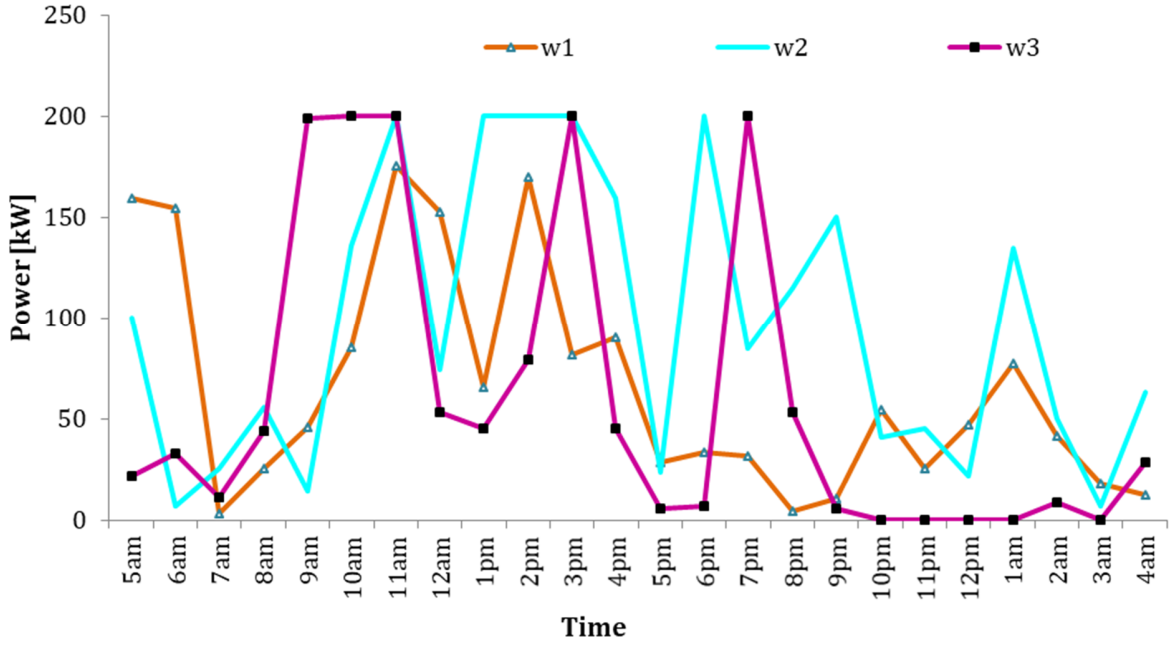

(b)

Fig. 4 (a) Power production curves of PV farms for each scenario, (b) 200 kW wind turbine power production curves for each scenario.

The residential end-users can be categorized into three groups by taking into account their lifestyle and as a result, this classification affects controllable appliances' operational period and the arrival-departure time of the EVs. The corresponding inflexible load profiles of each residential end-user type is determined considering commonly used domestic appliances' nominal power and duration of usage as portrayed in Fig. 3. Office building and pet production plants are selected as commercial and industrial premises, respectively. It should be highlighted that industrial end-users have great potential in terms of incorporating DR programs for utilizing their energy reduction capability. However, it is assumed that the industrial premise has fixed loads and it is not possible to change its power curve in this study. On the supply side, it is considered that MG includes wind turbines and PV farms with different generation capacities.

Wind speed, temperature, and irradiance values are taken from National Renewable Energy Laboratory and afterward, power production curves of DGs are obtained based on real data as depicted in Fig. 4 (a) and Fig. 4 (b) [44]. In this stochastic framework, the scenarios are created assuming equal probability occurrences same as the other literature studies [45]-[46]. The PV generation is taken into consideration 4 different scenarios (called as $v_1 - v_4$) for both 100 kW and 70 kW PV farms. Also, in order to assess the uncertain behaviour of wind production, 3 different scenarios are generated (called as $w_1 - w_3$) for both 200 kW and 300 kW wind turbines. After combining PV and wind scenarios, 12 different scenarios are obtained to get accurate results that reflect the stochastic programming nature of the system as given in Table 2. It should also be reminded that the proposed methodology is appropriate for applying the desired number of scenarios.

All residential and commercial end-users are assumed to be equipped with EVs which can only allow grid-to-vehicle (G2V) power flow and the suitable EVs to satisfy the needs of the residential end-users are selected on the market [47]. BMW i3, Volkswagen E-Golf, or Chevy Volt can be preferred by any residential end-user. On the contrary, Ford Transit Jumbo is the single option for commercial end-users allowing 90 kW charging power [48], which is evaluated as fast charging. The specifications of these vehicles are presented in Table 3. Arrival and departure times along with DR horizon are directly related to the end-user type and its behaviour.

In order to testify only how different charging strategies change proposed optimal energy management response as well as power losses, this issue is taken into consideration in different case studies. TSCM and DCCM methods are suggested for the residential and commercial end-users' flexible load of AC to utilize its energy reduction capability in the considered concept. In the DCCM DR program, load serving entity (LSE) can directly switch on/off ACs and determines the scheduling periods of TCLs while satisfying end-user's comfort requirements for aiding to the minimization of losses. On the other side, according to the given data in Table 4, AC's thermostat set-point is controlled between 25℃ and 26℃ at different time periods for every type of end-users in TSCM mode. Also, the same structural parameters are adopted for clarity and simplicity while assuming that all commercial and residential buildings are identical. The relevant data for commercial end-users are summarized in Table 5 and those for residential end-users are taken from [49].

Table 2: Created Scenarios for Case Studies

PV↓ \ Wind →	w_1	w_2	w_3
v_1	Scenario 1	Scenario 2	Scenario 3
v_2	Scenario 4	Scenario 5	Scenario 6
v_3	Scenario 7	Scenario 8	Scenario 9
v_4	Scenario 10	Scenario 11	Scenario 12

Table 3: Specifications of the Electric Vehicle, Renewable Energy Sources and Common Storage System

	Staff service	**Energy Storage System**
Battery capacity[kWh]	51.2	350
Charging/discharging rate [kW]	90	100
Charging/discharging efficiency [%]	95	95
Initial SOE [%]	30	350
Minimum SOE [%]	20	50
Wind Installation	Wind turbine I [kW]	Wind turbine II [kW]
	200	300
PV Installation	PV farm I [kW]	PV farm II [kW]
	100	70

Table 4: Various Temperature Values used for Houses

Parameter	**Quantity**	**Unit**	**Parameter**	**Quantity**	**Unit**
$T^{res,desired}$	20	℃	$S^{res,up}$	1	℃
$T^{res,up}$	4	℃	$S^{res,down}$	1	℃
$T^{res,down}$	3	℃			

Table 5: Structural Parameters of the Commercial End-Users

Parameter	**Value**	**Units**	**Parameter**	**Value**	**Units**
Office length	51.3	m	Windows area	1.615	m^2
Office width	16	m	Wall thermal coefficient	359.57	$\frac{J}{\mathrm{h} \cdot m \cdot ℃}$
Office height	3.6	m	Window thermal coefficient	2808	$\frac{J}{\mathrm{h} \cdot m \cdot ℃}$
Angle of roof	30	°	Window thickness	0.1	m
Window number	15	-	Wall Thickness	0.2	m

DLC-based DR strategies are mainly targeted at maximizing the penetration and utilization of RESs with the objective of minimizing total losses while remaining within the comfort and operational constraints. Regarding the air density and its thermal capacity, which are normally related to its thermodynamic properties (temperature, pressure, etc.), the standard values are used as given in [49] while considering them as constant. With respect to AC rated power, 2 kW and 10 kW are chosen for residential houses and commercial buildings, respectively. Also, a coefficient-of-performance (COP) of 2 is assumed for ACs.

3.2 Simulation Results and Discussion

To investigate the capability of the developed stochastic programming-based algorithm, it is applied to a five-node sample distribution system for a grid-connected MG and different case studies are performed to analyze the operational behaviour of EMS. Seven case studies are considered in this study as follows:

- **Base Case:** Flexible loads are unavailable. EVs and ACs operational periods are determined deterministically.
- **Case-2:** EVs are used as DR source and controlled at both residential and commercial end-users.
- **Case-3:** Fast charging is used for the EV of commercial end users in addition to the conditions in Case-2.
- **Case-4:** Besides EVs, residential end-users' flexible load of ACs are controlled by EMS.
- **Case-5:** Fast charging is used for the EV of commercial end users in addition to the conditions in Case-4.
- **Case-6:** ACs of commercial and residential end-users together is controlled.
- **Case-7:** Fast charging is used for the EV of commercial end users in addition to the conditions in Case-6.

The substation node power-energy balance comprising of drawn energy from the upstream grid, energy losses in the branches, injected energy to the upstream grid and power flow from Node 1 to other nodes are depicted in Fig. 5 for the Case 7 under Scenario 4. Fig. 6 graphically presents the power balance composed of l_1 and l_2 commercial premises' inflexible and flexible loads consumption, PV production and power flow between upstream grid and Node 2 for the Scenario 4. In the case studies, EVs having similar specifications are considered for commercial end-users for simplicity, and two charging strategies are taken into consideration in order to investigate its impact on the system. Arrival and departure time of the l_1 and l_2 EVs are assumed to be 9 am-6 pm, and 10 am-7 pm, respectively. Even though the EVs are connected to Node 2 in a large period of the time, they are charged for a relatively small period only during 12 am to 3 pm. During these periods, the commercial users' inflexible load doesn't reach to its highest value while both PV output powers are continuously increasing, as depicted in Fig. 6. It is observed that ACs are operated intermittently from 11 am to 2 pm, 5 pm to 6 pm and lastly 8.30 am to 8.55 am in the reference scenarios depending on the PV power output and fixed load of commercial premises. At certain conditions, it is necessary to operate them to prevent comfort violation while EMS sends the signals so as to reduce losses at different conditions. On the other hand, ACs are permanently operated from 12.10 am to 12.35 am even though the inside temperature is within the normal range. This is caused by the fact that PV power production reaches its maximum value and also inflexible load decreases.

Fig. 7 (a) shows that ESS is continuously discharging to cover the electricity demand of residential premises by supplying 350 kWh energy to the system. Since the minimum SOE of the ESS is considered as 50 kWh, a smaller amount of power is used for discharging when losses reduce. Wind turbines cannot generate sufficient power in Scenario 4 as shown in Fig. 7 (b) and as a result, this demand should be covered by the upstream grid. Thus, the mentioned problem leads to an increase in power flowing from the upstream grid to the nodes and in losses according to the loss function.

Fig. 8 shows the power balance at Node 5 including total inflexible load, different types and numbers of residential end-users' EVs charging power, and ACs demand for Case 7 in Scenario 4. The residential end-users are divided into three types and this separation has an effect on the departure and arrival times of EVs and ACs operational period. Since no DG unit is connected to Node 5, the power need should be met by upstream grid or common ESS.

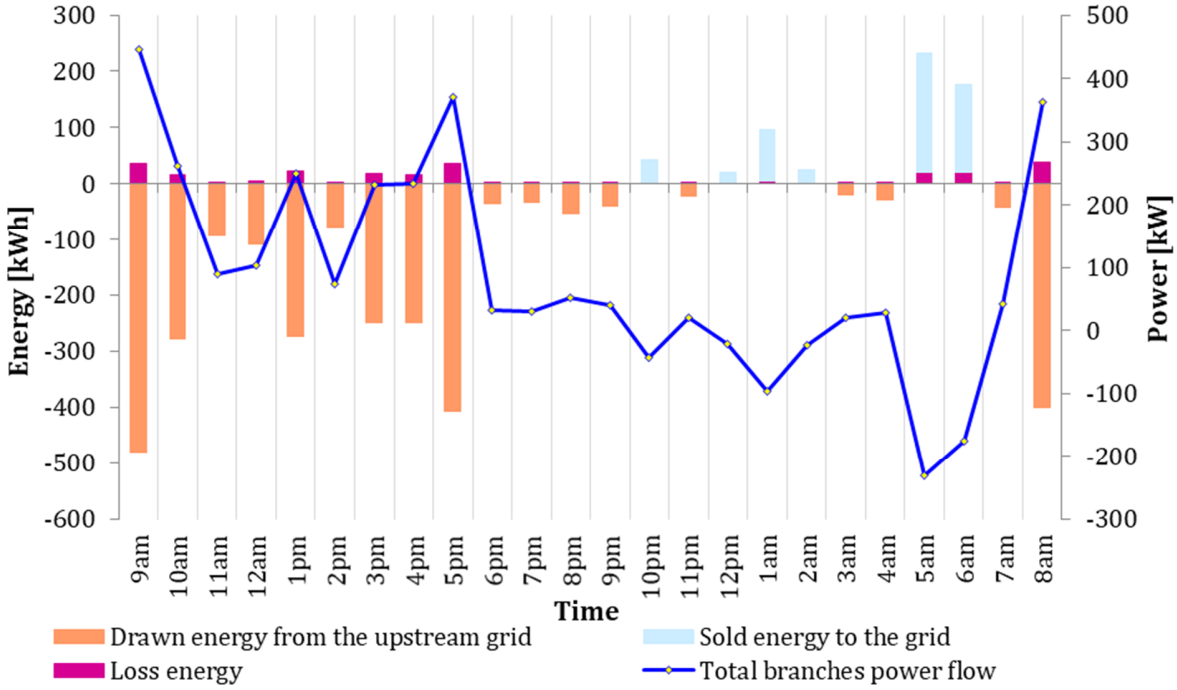

Fig. 5. Power-energy balance for Case-7 Scenario 4 at Node 1.

In order to simplify interpretation of the results for the considered 12 scenarios, Fig. 9 (a) is depicted to show the variations of the drawn power from Node 1. The line in the middle of the boxes presents the median of the supplied power for all scenarios during the day. The median separates the data into two parts which are called the first and third quartiles. Lastly, whiskers show the maximum and minimum power values with the end of the vertical lines.

For example, the drawn power varies between 182 kW to 610 kW; 25% of the data is lower than 244 kW, while 25% of the data is greater than 548 kW at 9 am considering all possibilities. It is clear that the supplied power has increased from 8 am to 5 pm depending on the power need of industrial/commercial premises and DG's energy production. On the other hand, it reached its minimum values due to the closure of these facilities and high wind energy production from 6 pm to 7 am. Excess energy has been injected into the upstream grid and there is no need for matching electricity demand by the upstream grid at these mentioned periods. Fig. 9 (b) shows loss variations in the branches. It is clearly seen that dramatically different results are obtained in the variations of loss energy at particularly 9 am, 6 pm, and 7 pm compared to the other periods.

Actually, they all occur because of different reasons, but box-whisker graphs enable the interpretation of all conditions as the first-seen. At 9 am, the ever-increasing power demand of the industrial premise leads to increasing fb_3 power flow through the upstream grid to Node 4 in some scenarios in which wind turbines production is low. Secondly, fb_1 power flow increases since PV farms are unable to meet the commercial premises' high electricity demand at this time and as a result, losses are sufficiently high. Thus, 50% of the data is higher than 35 kWh, which can be evaluated as an unnatural event. At 6 pm, although the median is around 2 kWh, it is seen that 25% of the obtained values are greater than 48 kWh. The reason for high deviations can be explained that DG's power production reaches the maximum values for fewer scenarios while nodes' demand decreases in the corresponding time periods as mentioned before and also similar conditions caused to rise in the lost energy at 7 pm. Consequently, it is indicated that the DG system capacity planning is a critical issue and has a non-negligible effect on the system operation considering the objective function.

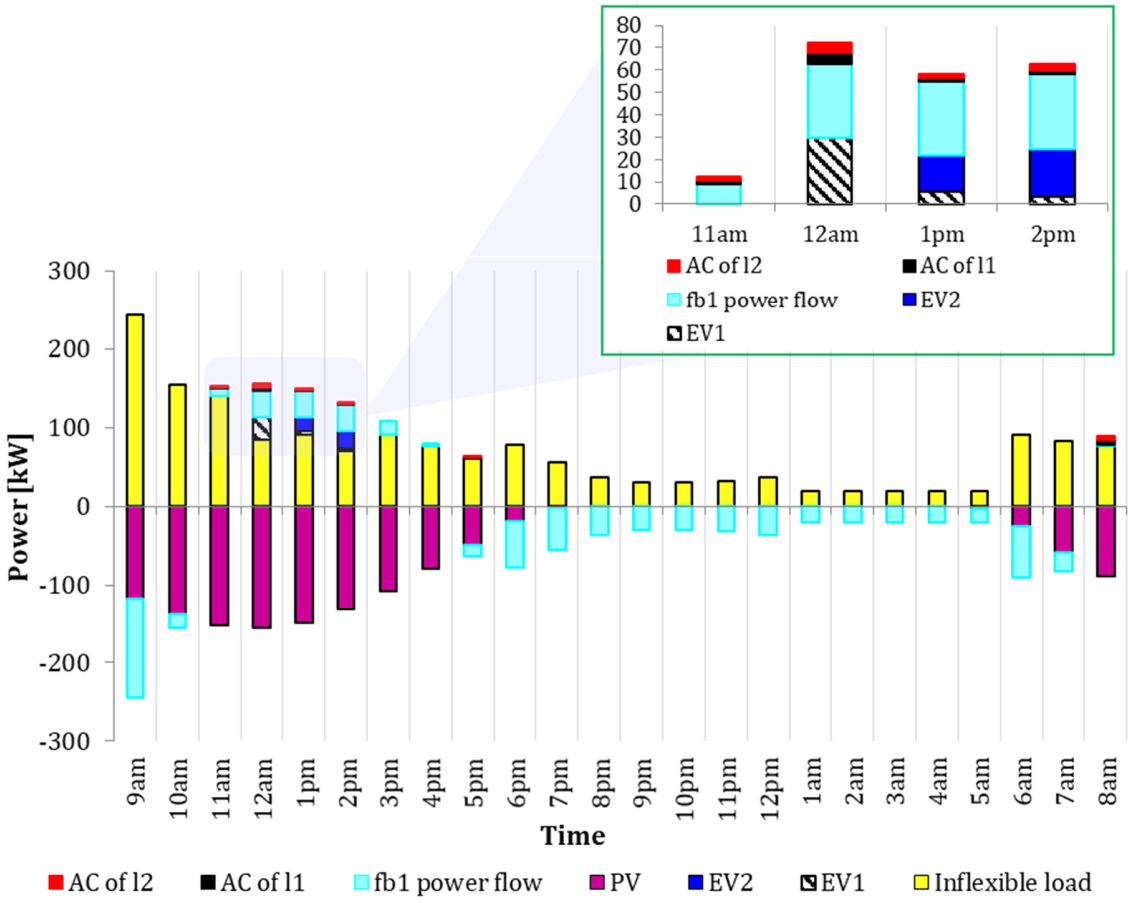

Fig. 6. Power balance for Case-7 Scenario 4 at Node 2.

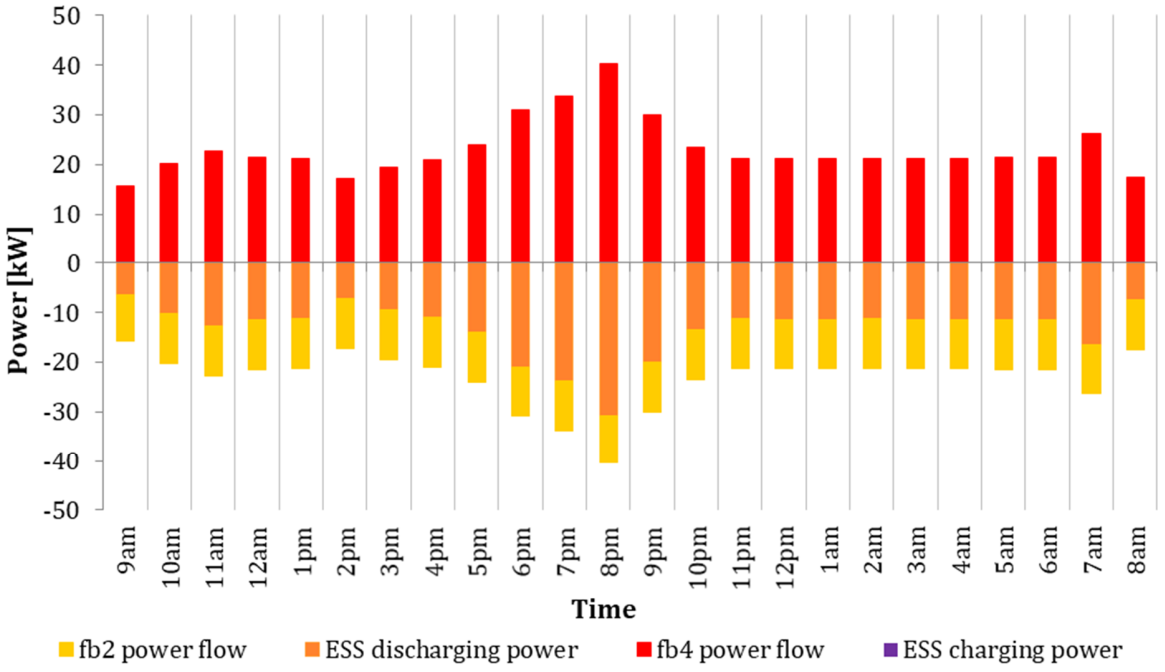

(a)

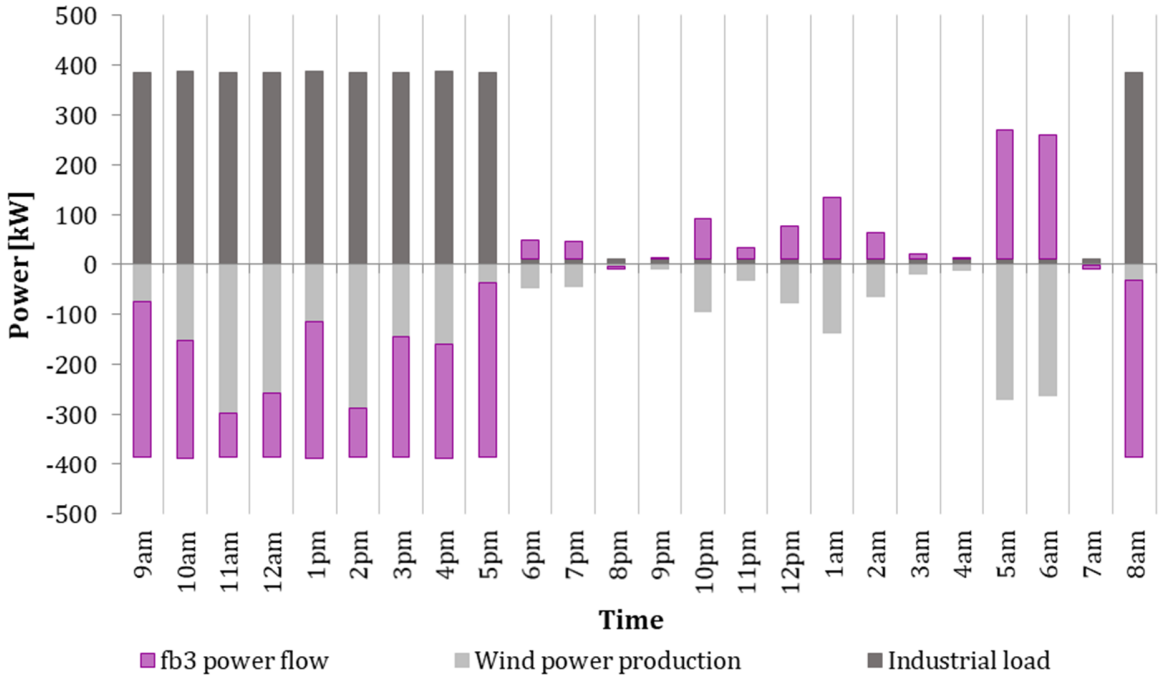

(b)

Fig. 7 (a) Power balance for Case-7 Scenario 4 at Node 3, (b) Power balance for Case-7 Scenario 4 at Node 4.

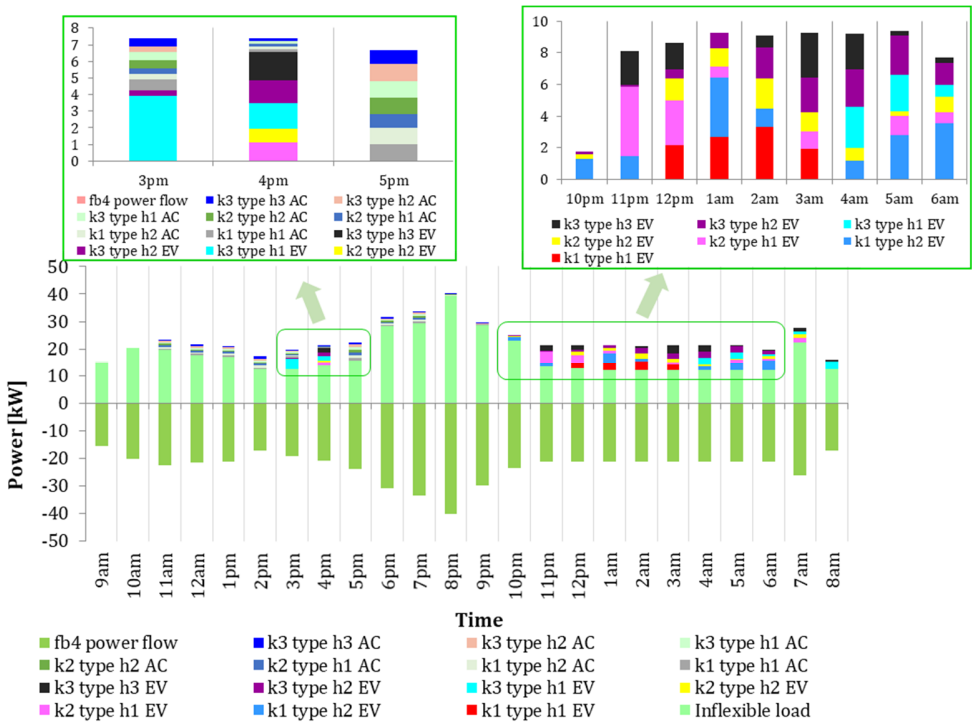

Fig. 8. Power balance for Case-7 Scenario 4 at Node 5.

Table 6 encapsulates the Base Case together with six different case studies (which are mentioned before) assessed in this study by taking into account the effect of the flexible appliance on the economic operation of MG by incorporating 12 scenarios. It may be indicated that the planning of charging periods of EVs and operational periods of ACs have a significant impact on the losses of the smart MG concept in this scenario-based approach. Even if only residential and commercial EVs' are controlled by the operator, nearly a 1.98% drop is achieved in the loss energy for Case 2. When the fast charging option is investigated, it is deduced from the table that this offers more flexibility and lower energy losses happened in Case 3 compared to Case 2, genuinely.

For the sake of clarity, there are supposed to be seven residential end-users in this MG structure and they are equipped with ACs which are controlled by the operator in Case 4 and Case 5. Even though the number of DR resources is not so many, there is a quietly considerable reduction that has been provided with the developed algorithm.

Furthermore, Cases 6 and 7 enable to reshape ACs and EVs demand curve while obtaining the lowest losses together with fast charging option. Although the number of controllable appliances is not so many, a 2.65% reduction is accomplished only by adjusting their periods. Hence, controllable loads play a critical role and present operational flexibility to the LSE via DR programs.

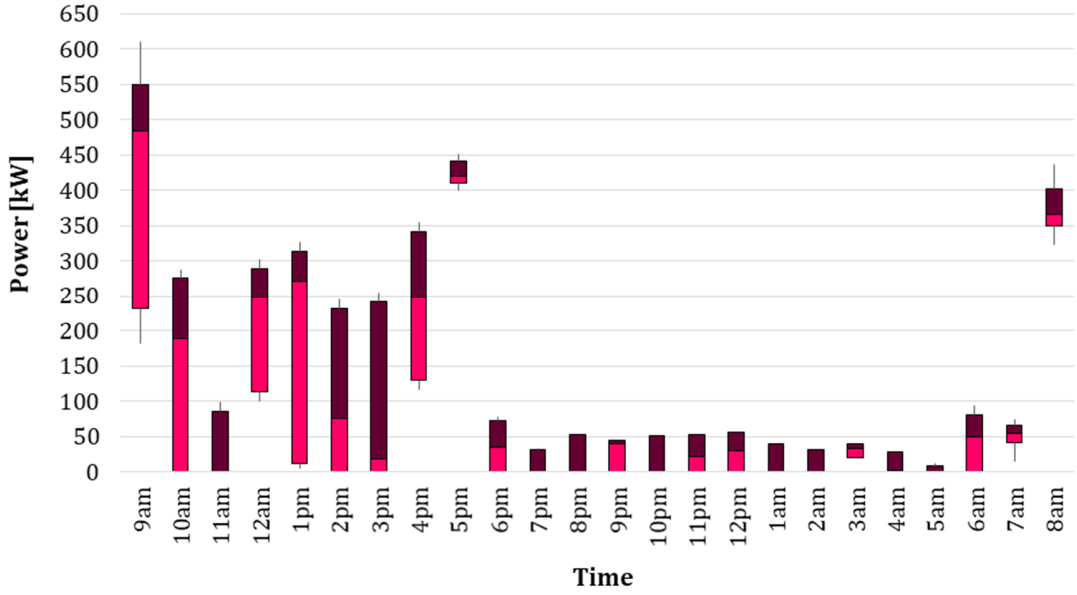

(a)

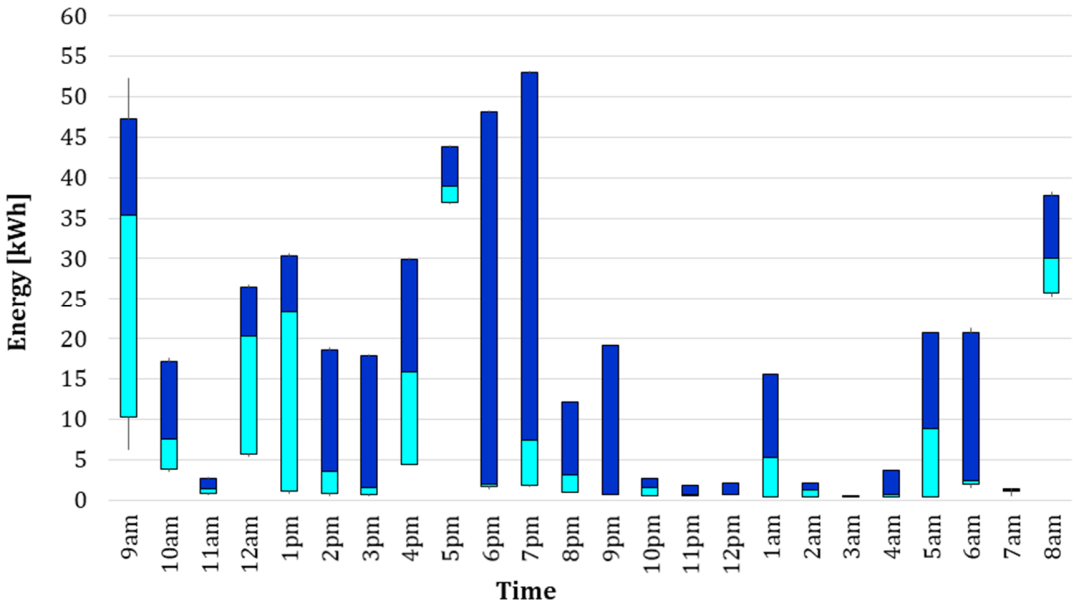

(b)

Fig. 9 (a) The drawn power variations from the slack bus for 12 scenarios in Case, (b) The loss energy variations for 12 scenarios in Case 7.

Table 6: The Energy Loss in the Branches for Seven Case Studies in a Stochastic Model

Case Study	Losses [kWh]	Loss Reduction [%]
Base Case	3264.392	Base Case
Case 2	3199.647	1.98
Case 3	3198.508	2.02
Case 4	3192.871	2.19
Case 5	3191.729	2.22
Case 6	3178.334	2.63
Case 7	3177.877	2.65

3.3 Comparison with the Deterministic Approach

In the literature, a considerable amount of successful studies have used deterministic modelling as a benchmark for a comparative performance evaluation of stochastic approaches from different points of view [10], [50]. Thus, in this subsection, a deterministic approach is utilized as a base methodology for the purpose of benchmarking the benefits of the stochastic formulation in the optimal operation of MG. A comparison is conducted to demonstrate the effectiveness of the proposed approach using the same test system and parameters. The test system will help readers understand the philosophy behind the algorithm by enabling them to investigate almost all components' operational behaviours, clearly. Also, it is proved that the developed energy management strategy is working properly. In order to better understand this analysis, the loss reduction value (objective function) is determined as an index in terms of showing which method is best for system planning.

Fig. 10 (a) graphically presents the hourly total consumption consisting of residential premises (fixed and flexible loads), commercial premises (fixed and flexible loads) and industrial premise. Also, PV and wind data used in this deterministic approach are depicted with ESS discharging power as well as transferred power from upstream grid. To further compare the performances of MG energy management strategies, Fig. 10 (b) is depicted to show daily power losses for both stochastic and deterministic approaches. By comparing Figs. 10 (a) and 10 (b), it can be deduced that the power loss is quite high because of the high wind production and low load level, especially at 6 pm, 9 pm and 1 am under a deterministic model. From 1 pm to 4 pm, the larger power loss occurs in the stochastic model, because average (multiplied with equal probabilities of scenarios) wind and PV production is lower than the data used in the deterministic model.

Table 7 presents the objective function values under a deterministic model and it is compared with Table 6 for indicating the benefits of using a scenario-based stochastic approach. It can be seen that the proposed scheme has much better performance in terms of achieving low power losses. Note that, obtaining approximately 2.65% loss reduction does not only show superiority of using one approach over the other, but also indicates that this value can be even increased considering a larger MG architecture. Besides, all 12 real-world scenarios are capable of capturing the uncertainties better than a deterministic framework, providing a more realistic system scheduling. Moreover, the decisions are more accurate and close to what can be expected in practical implementations. It is worth mentioning that uncertainties have great impacts on MG operation scheduling process. The underestimation or overestimation can cause infeasible, uneconomical and insufficient system planning that should be avoided. Therefore, a comprehensive stochastic optimization model can be helpful here to provide effective management strategies as well as economically and environmentally acceptable designs.

Table 7: The Energy Loss in the Branches for Seven Case Studies in a Deterministic Model

Case Study	**Losses [kWh]**	**Loss Reduction [%]**
Base Case	3444.717	Base Case
Case 2	3373.463	2.06
Case 3	3372.365	2.10
Case 4	3366.786	2.26
Case 5	3365.611	2.29
Case 6	3353.126	2.65
Case 7	3352.652	2.67

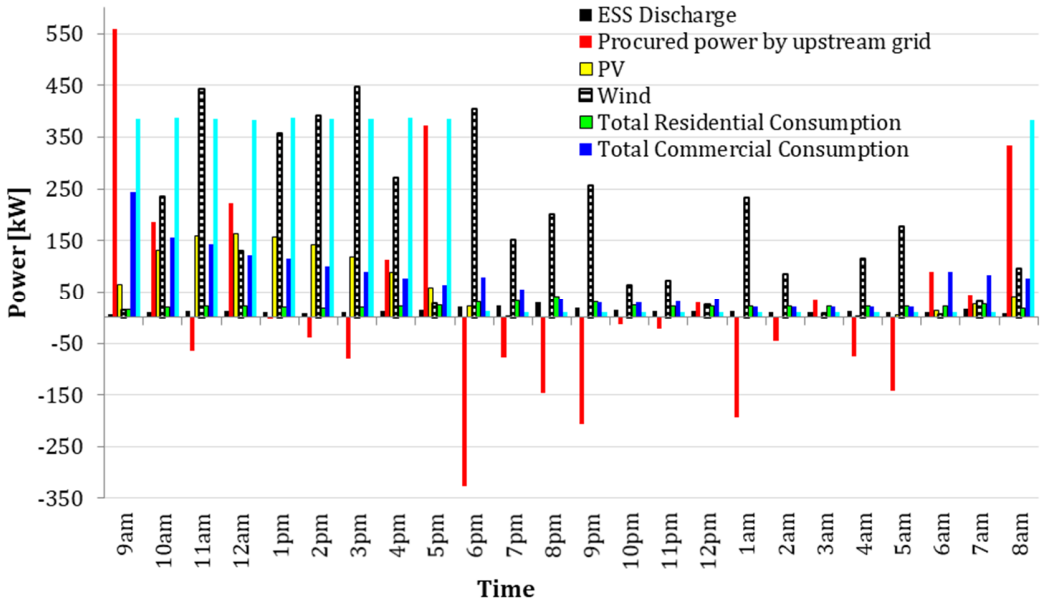

(a)

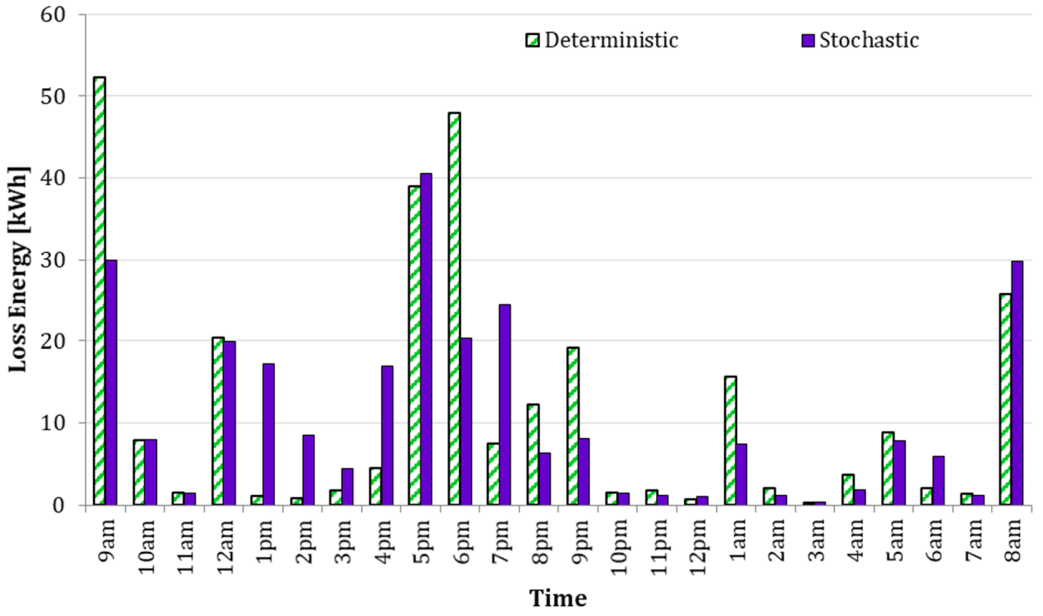

(b)

Fig. 10 (a) Power dispatch for a 24 h period using wind, PV, ESS, upstream grid, and end-user premises in Case 7, (b) Hourly energy losses over one day under deterministic and stochastic approaches in Case 7.

4. Conclusion

In this study, a scenario-based EMS framework was proposed by taking the stochastic nature of wind and PV systems into consideration for grid-connected MGs. In this structure, a DLC-based DR program was integrated into the EMS to schedule the operational period of ACs and charging/discharging periods of common ESS. Furthermore, EVs were considered with the G2V mode option. All the aforementioned units were formulated based on a MILP framework for minimizing branches' total losses and different case studies were conducted by considering different scenarios in order to investigate the effectiveness of the proposed algorithm. The detailed MILP-based mathematical model makes it possible to ensure global optimality. Even though a minute-scale time granularity is selected for making realistic assumptions, the energy management strategy performs effectively in terms of scheduling multi parties in an optimal fashion. It was observed that the operation of the system components should not be evaluated independently in MG operation. The obtained simulation results proved the efficacy of the centralized loss reduction maximization oriented energy management framework to yield benefits for the distribution system operators. Compared to the case studies without considering DR strategy for EV and AC in a 24-hour time horizon operation, the best optimization results were obtained with a higher DR participation level. Flexible load profiles were strongly related to DG power output and all controllable appliances were operated to utilize this power as much as possible when it reaches the maximum value, surely satisfying the operational and comfort constraints. Also, using fast charging option enables to adjust the charging power of the EV on large scale and as a result, this offers improved flexibility. Increased DG production, on the other hand, reduced the amount of energy drawn from the upstream grid and had a significant impact on the losses when energy is consumed where it is generated. However, it was obtained that the DG system capacity planning is a vital issue in the economic operation of MG and has a non-negligible effect on the system operation considering the objective function. Furthermore, the presence of the common ESS in the MG structure provided operational flexibility, and this dynamic component's charging/discharging periods were determined by the proposed EMS structure according to the loss function. Even though the number of considered controllable appliances is not so many and the test system is relatively small-scale, approximately 2.65% loss reduction was obtained. Overall, it can be deduced that the stochastic approach outperformed the deterministic approach in terms of achieving loss reduction and capturing the uncertainties in MG operation. The presented methodology can be extended in various ways such as (i) applying the proposed method to a larger scale distribution system including shiftable appliances (washing machine, dishwasher, etc.), (ii) considering the power exchanges between a group of MGs, (iii) investigating the benefits of different DR strategies on the proposed system structure, and (iv) adopting a different objective function such as minimizing the total cost, minimizing comfort violation of end-users and maximizing the load-serving entity's profit, for analyzing the performance of the proposed algorithm from different aspects.

Acknowledgment

The work of Ozan Erdinç is supported by the Turkish Science Academy (TUBA), under the Distinguished Young Scientist Programme (GEBIP), and by The Scientific and Technological Research Council of Turkey (TUBITAK), under project Grant 116E115. Also, João P. S. Catalão acknowledges the support by FEDER funds through COMPETE 2020 and by Portuguese funds through FCT, under POCI-01-0145-FEDER-029803 (02/SAICT/2017).

References

[1] A. T. Eseye, D. Zheng, H. Li, and J. Zhang, “Grid-price dependent optimal energy storage management strategy for grid-connected industrial microgrids,” IEEE Green Technol. Conf., pp. 124–131, 2017.

[2] J. A. Peças Lopes, C. L. Moreira, and A. G. Madureira, “Defining control strategies for microgrids islanded operation,” IEEE Trans. on Power Systems., vol. 21, pp. 916-924. May.2006.

[3] C. Ahn and H. Peng, “Decentralized voltage control to minimize distribution power loss of microgrids,” IEEE Trans. Smart Grid, vol. 4, no. 3, pp. 1297–1304, 2013.

[4] K. Meng, D. Wang, Z.Y. Dong, X. Gao, Y. Zheng, and K.P. Wong, “Distributed control of thermostatically controlled loads in distribution network with high penetration of solar PV,” CSEE Journal of Power and Energy Systems., Vol. 3, pp. 53-62, March 2017.

[5] A. A. Zaidi, F. Kupzog, T. Zia, and P. Palensky, “Load recognition for automated demand response in microgrids,” IECON in Proc. 2016 Industrial Electron. Conf., pp. 2442–2447.

[6] M. Khederzadeh, “Frequency control of microgrids by demand response,” 2012 International Conf. on Electricity Distribution., pp. 1–4.

[7] A. Chaouachi, R.M. Kamel, R. Andoulsi, and K. Nagasaka, “Multiobjective intelligent energy management for a microgrid,” IEEE Trans. Ind. Electron., vol. 60, no. 4, pp. 1688–1699, Apr. 2013.

[8] S. X. Chen and H. B. Gooi, “Jump and shift method for multi-objective optimization,” IEEE Trans. Ind. Electron., vol. 58, no. 10, pp. 4538–4548, Oct. 2011.

[9] Z. Li and M. Ierapetritou, “Process scheduling under uncertainty: Review and challenges,” Comput. Chem. Eng., vol. 32, no. 4–5, pp. 715–727, 2008.

[10] W. Su, J. Wang, and J. Roh, “Stochastic energy scheduling in microgrids with intermittent renewable energy resources,” IEEE Trans. Smart Grid., vol. 5, no. 4, pp. 1876–1883, 2014.

[11] Y. M. Atwa and E. F. El-Saadany, "Probabilistic approach for optimal allocation of wind-based distributed generation in distribution systems," in IET Renewable Power Generation., vol. 5, no. 1, pp. 79-88, January 2011. doi: 10.1049/iet-rpg.2009.0011

[12] A. Soroudi and M. Ehsan, “A possibilistic-probabilistic tool for evaluating the impact of stochastic renewable and controllable power generation on energy losses in distribution networks-A case study,” Renew. Sustain. Energy Rev., vol. 15, no. 1, pp. 794–800, 2011.

[13] C. Haifeng, X. Yuan, L. Tao, and L. Zhouhong, “Parameter sensitivity analysis of economic operation cost of CCHP-typed microgrid,” 2nd IEEE Conf. Energy Internet Energy Syst. Integr., pp. 1–6, 2018.

[14] H. Afshar, Z. Moravej, and M. Niasati, “Modeling and optimization of microgrid considering emissions,” Smart Grid Conf. 2013, SGC 2013, pp. 225–229, 2013.

[15] S. Kutaiba, D. N. Hung, J. Shantha, M. Thair, “Multiobjective intelligent energy management optimization for grid-connected microgrids,” 2018 IEEE Int. Conf. on Environment and Electrical Engineering, 2018.

[16] D. Olivares, L. Marin, C. Canizares, F. Avila, and D. Saez, “Fuzzy prediction ınterval models for forecasting renewable resources and loads in microgrids,” IEEE Trans. Smart Grid., vol. 6, no. 2, pp. 548–556, 2014.

[17] A. Omishore and L. Puklický, “Fuzzy probabilistic models, uncertainty and structural reliability,” no. March, 2009.

[18] A. Hussain, V.H. Bui, H.M. Kim, “Robust optimization-based scheduling of multi-microgrids considering uncertainties,” Energies., 9. 1-21, 2016. 10.3390/en9040278,

[19] D. B. Shmoys and C. Swamy, “Stochastic optimization is (almost) as easy as deterministic optimization,” pp. 228–237, 2004.

[20] Y. Xiang, J. Liu, and Y. Liu, “Robust energy management of microgrid with uncertain renewable generation and load,” IEEE Trans. Smart Grid., vol. 7, no. 2, pp. 1034–1043, 2016.

[21] W. Shi, X. Xie, C. Chu, and R. Gadh, “Distributed optimal energy management in microgrids,” IEEE Trans. on Smart Grid., vol. 6, pp. 1137-1146, Dec. 2014.

[22] S. Conti, R. Nicolosi, S. A. Rizzo, and H. H. Zeineldin, “Optimal dispatching of distributed generators and storage systems for MV islanded microgrids,” IEEE Trans. on Power Delivery., vol. 27, pp. 1243–1251, July. 2012.

[23] F. S. Gazijahani, A. A. Abadi, H. Hosseinzadeh, and J. Salehi, “Optimal day-ahead power scheduling of microgrids considering demand and generation uncertainties,” 2017 Iranian Conf. on Electrical Engineering., pp. 943–948.

[24] M. Farrokhifar, “Optimal operation of energy storage devices with RESs to improve efficiency of distribution grids; Technical and economical assessment,” Int. J. Electr. Power Energy Syst., vol. 74, pp. 153–161, 2016.

[25] K. Dietrich, J. M. Latorre, L. Olmos, and A. Ramos, “Demand response in an isolated system with high wind integration,” IEEE Trans. on Power Systems., vol. 27, pp. 20-29, February 2012.

[26] M. A. López, S. Martín, J. A. Aguado, and S. De La Torre, “Optimal microgrid operation with electric vehicles,” 2011 IEEE PES Innovation Smart Grid Technology Conf. Europe., pp. 1–8.

[27] D. Hanane, Q. Ahmed, A. Dessaint, Louis, “Peak load reduction in a smart building integrating microgrid and V2B-based demand response scheme,” IEEE Systems Journal., pp. 1-9, 2018.

[28] S. A. Pourmousavi, M. H. Nehrir, and R. K. Sharma, “Multi-timescale power management for islanded microgrids including storage and demand response,” IEEE Trans. on Smart Grid., vol. 6, pp. 1185–1195, May. 2015.

[29] A. G. Tsikalakis, and N. D. Hatziargyriou, “Centralized control for optimizing microgrids operation,” IEEE Trans. on Energy Conversion., vol. 23, pp.241-248, March 2008.

[30] V. Bui, A. Hussain, and H. Kim, “A multiagent-based hierarchical energy management strategy for multi-microgrids considering adjustable power and demand response,” IEEE Trans. on Smart Grid., vol. 9, PP.1323-1333, March 2018.

[31] W. Alharbi, and K. Bhattacharya, “Demand response and energy storage in MV islanded microgrids for high penetration of renewables,” IEEE 2013 Electrical Power & Energy Conference (EPEC)., May. 2014.

[32] M. Alipour, B. Mohammadi-Ivatloo, and K. Zare “Stochastic scheduling of renewable and CHP-based microgrids,” IEEE Trans. Industrial Informatics, vol. 11, no. 5, pp.1049-1058, October. 2015.

[33] S. A. Arefifar, M. Ordonez, and Y. A. R. I. Mohamed, “Energy management in multi-microgrid systems - development and assessment,” IEEE Trans. Power Syst., vol. 32, no. 2, pp. 910–922, 2017.

[34] J. Yang and C. Su, “Robust optimization of microgrid based on renewable distributed power generation and load demand uncertainty,” vol. 223, 2021.

[35] P. Hajiamoosha, A. Rastgou, S. Bahramara, and S. M. Bagher Sadati, “Stochastic energy management in a renewable energy-based microgrid considering demand response program,” *Int. J. Electr. Power Energy Syst.*, vol. 129, no. April 2020, p. 106791, 2021, doi: 10.1016/j.ijepes.2021.106791.

[36] S. E. Ahmadi and N. Rezaei, “A new isolated renewable based multi microgrid optimal energy management system considering uncertainty and demand response,” *Int. J. Electr. Power Energy Syst.*, vol. 118, no. December 2019, 2020, doi: 10.1016/j.ijepes.2019.105760.

[37] R. S. Kumar, L. P. Raghav, D. K. Raju, and A. R. Singh, “Intelligent demand side management for optimal energy scheduling of grid connected microgrids,” *Appl. Energy*, vol. 285, no. January, 2021, doi: 10.1016/j.apenergy.2021.116435.

[38] M. A. Mosa and A. A. Ali, “Energy management system of low voltage dc microgrid using mixed-integer nonlinear programing and a global optimization technique,” *Electr. Power Syst. Res.*, vol. 192, no. November 2020, 2021, doi: 10.1016/j.epsr.2020.106971.

[39] F. Khavari, A. Badri, and A. Zangeneh, “Energy management in multi-microgrids considering point of common coupling constraint,” *Int. J. Electr. Power Energy Syst.*, vol. 115, no. August 2019, 2020, doi: 10.1016/j.ijepes.2019.105465.

[40] T. Adefarati, R. C. Bansal, M. Bettayeb, and R. Naidoo, “Optimal energy management of a PV-WTG-BSS-DG microgrid system,” *Energy*, vol. 217, 2021, doi: 10.1016/j.energy.2020.119358.

[41] H. Karimi and S. Jadid, “Optimal energy management for multi-microgrid considering demand response programs: A stochastic multi-objective framework,” *Energy*, vol. 195, pp. 1–13, 2020, doi: 10.1016/j.energy.2020.116992.

[42] F. De Angelis, M. Boaro, D. Fuselli, S. Squartini, F. Piazza, Q. Wei, “Optimal home energy management under dynamic electrical and thermal constraints,” IEEE Trans. on Ind. Inform., vol. 9, pp. 1518-1527, August. 2013.

[43] N. G. Paterakis, S. F. Santos, J. P. S. Catalão, O. Erdinc, and A. G. Bakirtzis, “Coordination of smart-household activities for the efficient operation of intelligent distribution systems,” 2015 IEEE PES Innovation Smart Grid Technology Conf. Europe., pp. 1-6.

[44] [Online]. Available: https://midcdmz.nrel.gov/.

[45] Şengör, İ., Kılıçkıran, H. C., Akdemir, H., Kekezoğlu, B., Erdinc, O., & Catalao, J. P., “Energy management of a smart railway station considering regenerative braking and stochastic behaviour of ESS and PV generation,” IEEE Trans. Sustain. Energy., 9(3), 1041-1050, 2018.

[46] Şengör, I., Erdinç, O., Yener, B., Taşcikaraoglu, A., Catalão, J. P., “Optimal energy management of EV parking lots under peak load reduction based dr programs considering uncertainty” IEEE Trans. on Sustain. Energy., 2018. doi: 10.1109/TSTE.2018.2859186.

[47] N. G. Paterakis, O. Erdinc, I.N. Pappi, A. G. Bakirtzis, J.P.S. Catalão, “Coordinated operation of a neighborhood of smart households comprising electric vehicles, energy storage and distributed generation”, IEEE Trans. on Smart Grid., vol. 7, pp. 2736-2747, November. 2016.

[48] [Online]. Available: http://www.liotech.ru/ensmallford

[49] O. Erdinç, A. Taşcıkaraoglu, N. G. Paterakis, Y. Eren, and J.P.S. Catalão “End-User comfort oriented day-ahead planning for responsive residential HVAC demand aggregation considering weather forecasts,” IEEE Trans. on Smart Grid., vol. 8, pp. 362-372, January 2017.

[50] Z. Ding, W. J. Lee, and J. Wang, “Stochastic resource planning strategy to improve the efficiency of microgrid operation,” IEEE Trans. Ind. Appl., vol. 51, no. 3, pp. 1978–1986, 2014.

Appendix

The main nomenclature used throughout this study is stated in Table 1- 3.

Table 1: Sets and Indices

$b \in B$	Set of branches.
$c \in C$	Set of wind turbines.
$f \in F$	Set of PV farms.
$h \in H$	Set of residential end-users in each residential type.
$i \in I$	Set of nodes.
$k \in K$	Set of residential end-user types.
$l \in L$	Set of commercial end-user types.
$t \in T$	Set of time periods.
$v \in V$	Set of PV farms' scenarios.
$w \in W$	Set of wind turbines' scenarios.
$\Omega_i^i, \Omega_i^j \in \Omega_i^f$	Set of substation nodes.

Table 2: Parameters & Constants

c_a	Thermal capacity of air [kJ/kg · ℃].
CE^{ESS}	Charging efficiency of common ESS.
$CE_{k,h}^{EV,R}$	EV charging efficiency of type k residential end-user h.
$COP_{k,h}$	Coefficient-of-performance for type k residential end-user h.
DE^{ESS}	Discharging efficiency of ESS.
f_b^{max}	Flow limit of branch b [kW].
L_1^R	Residential length [m].
L_2^R	Residential premise width [m].
L_3^R	Residential premise height [m].
l_i	Element thickness [m].
M_a^R	Total mass of air for residential premises [kg].
N	Sufficiently large positive constant.
$P_{c,w,t}^{wind}$	Power generation for wind turbine in period t [kW].
$P_{f,v,t}^{pv}$	Power generation for PV farm in period t [kW].
$P_i^{f,max}$	Allowed maximum power limit for substation node [kW].
$P_{k,h,t}^{inf,R}$	Inflexible load of residential end-users [kW].
$P_{k,h}^{R,AC}$	Air conditioner rated power for residential end-users [kW].
$P_{l,t}^{inf,C}$	Inflexible load of commercial end-users [kW].
P_t^{ind}	Power consumption of industrial premise [kW].
$P_{v,t}^{pv,tot}$	Total PV power generation in period t [kW].
$P_{w,t}^{wind,tot}$	Total wind power generation in period t [kW].
$R^{ESS,ch}$	Charging rate of common ESS [kW].
$R^{ESS,dis}$	Discharging rate of common ESS [kW].
$R_{k,h}^{ch,R}$	EV charging rate for type k residential end-user h [kW].
$R_{k,h}^{eq}$	Equivalent thermal resistance of type k residential end-user h [h· ℃/J].
$SOE^{ESS,ini}$	Initial SOE of common ESS [kWh].
$SOE^{ESS,max}$	Maximum SOE of common ESS [kWh].
$SOE^{ESS,min}$	Minimum SOE of common ESS [kWh].
$SOE_{k,h}^{ini,R}$	EV initial SOE of type k residential end-user h [kWh].
$SOE_{k,h}^{max,rR}$	EV maximum SOE of type k residential end-user h [kWh].
$SOE_{k,h}^{min,R}$	EV minimum SOE of type k residential end-user h [kWh].
$SP_{k,h,t}^{R,AC}$	Air conditioner temperature set-point for type k residential end-user h in period t [℃].
t_1	Starting period of the contracted DR period for residential end-users.
t_2	Ending period of the contracted DR period for residential end-users.
$T_{k,h,r}^a$	EV arrival time of type k residential end-user h.
$T_{k,h,r}^d$	EV departure time of type k residential end-user h.
$T_{k,h}^{res,des}$	Desired comfort temperature level of type k residential end-user h [℃].
$T_{k,h}^{res,d}$	Maximum allowed temperature set-point decrease from the desired comfort temperature level of type k residential end-user h during DR event [℃].
$T_{k,h}^{res,u}$	Maximum allowed temperature set-point increase from the desired comfort temperature level of type k residential end-user h during DR event [℃].
T_t^a	Outdoor air temperature in period t [℃].
V_{res}	Volume of the residential premise [m^3].
Y_p	Y- Coordinate of point p that is used for approximation.
X_p	X- Coordinate of point p that is used for approximation.
π_w	Probability of scenario w.
π_v	Probability of scenario v.

Table 3: Decision Variables

$F_{b,v,w,t}$	Approximate value of the square of the power flow through branch b during period t [kW^2].
$f_{b,v,w,t}$	Active power flow of branch b during period t [kW].
$P_{b,v,w,t}^{loss}$	Power losses of branch b during period t [kW].
$P_{i,v,w,t}^{f,load}$	Active power provided by substation node during period t to cover the demand [kW].
$P_{i,v,w,t}^{f}$	Total active power provided by substation node during period t [kW].
$P_{k,h,v,w,t}^{EV,R}$	EV charging power of type k residential end-user h in period t [kW].
$P_{k,h,v,w,t}^{R,AC}$	Air conditioner power consumption of type k residential end-user h in period t [kW].
$P_{k,h,v,w,t}^{R}$	Consumed power of type k residential end-user h in period t [kW].
$P_{l,v,w,t}^{EV,C}$	EV charging power of type l commercial end-user in period t [kW].
$P_{l,v,w,t}^{C,AC}$	Air conditioner power consumption of type l commercial end-user in period t [kW].
$P_{l,v,w,t}^{C}$	Power consumption of type l commercial end-user in period t [kW].
$P_{v,w,t}^{ESS,ch}$	Charging power of common ESS in period t [kW].
$P_{v,w,t}^{ESS,dis,tot}$	Total ESS discharging power during period t [kW].
$P_{v,w,t}^{ESS,dis}$	Discharging power of common ESS during period t [kW].
$P_{v,w,t}^{ESS,ch,tot}$	Total charging power of common ESS during period t [kW].
$P_{v,w,t}^{C,tot}$	Total power consumption of commercial end-users during period t [kW].
$P_{v,w,t}^{R,tot}$	Total power consumption of residential end-users during period t [kW].
$P_{v,w,t}^{sell,grid}$	Power injected to upstream grid during period t [kW].
$SOE_{k,h,v,w,t}^{R}$	EV SOE of type k residential end-user h during period t [kWh].
$SOE_{v,w,t}^{ESS}$	SOE of common ESS during period t [kWh].
$S_{v,w,t}^{R,d}$	Deviation of residential end-user indoor temperature from the ideal point to down side during period t [℃].
$S_{v,w,t}^{R,u}$	Deviation of residential end-user indoor temperature from the ideal point to upper side during period t [℃].
$T_{k,h,v,w,t}^{r,R}$	Room temperature of type k residential end-user h [℃].
$u_{k,h,v,w,t}^{EV,R}$	Binary variable. 1 if EV is charging in period t; else 0.
$u_{k,h,v,w,t}^{R,AC}$	Binary variable. 1 if type k residential end-user h's air conditioner is operating in period t; else 0.
$u_{v,w,t}^{ESS}$	Binary variable. 1 if ESS is charging in period t; else 0.
$u_{v,w,t}^{grid}$	Binary variable. 1 if microgrid is drawing power from the upstream grid in period t; else 0.
$z_{b,v,w,t,p}$	SOS2 variables that are used to approximate the power losses.